centrations of about 55 M, a low K_M for the substrate has not been a necessity.

REFERENCES

Abramowicz, D. A., & Dismukes, G. C. (1984) *Biochim. Biophys. Acta 765*, 318–328.

Bowlby, N. R., & Frasch, W. D. (1986) *Biochemistry 25*, 1402–1407.

Bowlby, N. R., & Frasch, W. D. (1987) *Prog. Photosynth. Res. I.5*, 693–696.

Briantais, J.-M., Vernotte, C., Lavergne, J., & Arntzen, C. J. (1977) *Biochim. Biophys. Acta 461*, 61–74.

Brudvig, G. W., Casey, J. L., & Sauer, K. (1983) *Biochim. Biophys. Acta 723*, 366–371.

Casey, J. L., & Sauer, K. (1984) *Biochim. Biophys. Acta 767*, 21–28.

Cheniae, G. M., & Martin, I. F. (1970) *Biochim. Biophys. Acta 197*, 219–239.

Chung, S. I., & Folk, J. E. (1970) *J. Biol. Chem. 245*, 681–689.

Cleland, W. W. (1967) *Adv. Enzymol. Relat. Areas Mol. Biol. 29*, 1–32.

Cleland, W. W. (1970) *Enzymes (3rd Ed.) 2*, 1–65.

Cleland, W. W. (1977) *Adv. Enzymol. Relat. Areas Mol. Biol. 45*, 273–387.

Dismukes, G. C., & Siderer, Y. (1980a) *FEBS Lett. 121*, 78–80.

Dismukes, G. C., & Siderer, Y. (1980b) *Proc. Natl. Acad. Sci. U.S.A. 78*, 274–278.

Forbush, B., Kok, B., & McGloin, M. (1971) *Photochem. Photobiol. 14*, 307–321.

Frasch, W. D., & Cheniae, G. M. (1980) *Plant Physiol. 65*, 735–745.

Frasch, W. D., & Mei, R. (1987) *Biochim. Biophys. Acta 891*, 8–14.

Ghanotakis, D. F., & Yocum, C. F. (1986) *FEBS Lett. 197*, 244–248.

Ghanotakis, D. F., Babcock, G. T., & Yocum, C. F. (1985) *Biochim. Biophys. Acta 809*, 173–180.

Itoh, S., Yerkes, C. T., Koike, H., Robinson, H. H., & Crofts, A. R. (1984) *Biochim. Biophys. Acta 766*, 612–622.

Kok, B., Forbush, B., & McGloin, M. (1970) *Photochem. Photobiol. 11*, 457–475.

Metz, J. G., Wong, J., & Bishop, N. I. (1980) *FEBS Lett. 114*, 61–66.

Ono, T., Zimmermann, J. L., Inoue, Y., & Rutherford, A. W. (1986) *Biochim. Biophys. Acta 851*, 193–201.

Radmer, R., & Cheniae, G. M. (1977) in *Primary Processes in Photosynthesis* (Barber, J., Ed.) pp 303–348, Elsevier/North-Holland, Amsterdam.

Renger, G. (1972) *Biochim. Biophys. Acta 256*, 428–439.

Sandusky, P. O., & Yocum, C. F. (1984) *Biochim. Biophys. Acta 766*, 603–611.

Sandusky, P. O., & Yocum, C. F. (1986) *Biochim. Biophys. Acta 849*, 85–93.

Styring, S., & Rutherford, A. W. (1987) *Biochemistry 26*, 2401–2405.

Theg, S., Jursinic, P., & Homann, P. (1984) *Biochim. Biophys. Acta 766*, 636–646.

Velthuys, B., & Kok, B. (1978) *Biochim. Biophys. Acta 502*, 211–221.

Yerkes, C. T., & Crofts, A. R. (1983) *Biophys. J. 41*, 39A.

Zimmermann, J. L., & Rutherford, A. W. (1984) *Biochim. Biophys. Acta 767*, 160–167.

Steric Repulsion between Phosphatidylcholine Bilayers†

T. J. McIntosh,*,‡ A. D. Magid,‡ and S. A. Simon§

Departments of Anatomy, Anesthesiology, and Physiology, Duke University Medical Center, Durham, North Carolina 27710

Received April 22, 1987; Revised Manuscript Received June 15, 1987

ABSTRACT: The change in pressure needed to bring egg phosphatidylcholine bilayers into contact from their equilibrium separation in excess water has been determined as a function of both distance between the bilayers and water content. A distinct upward break in the pressure–distance relation appears at an interbilayer separation of about 5 Å, whereas no such deviation is present in the pressure–water content relation. Thus, this break is not a property of the dehydration process per se, but instead is attributed to steric repulsion between the mobile lipid head groups that extend 2–3 Å into the fluid space between bilayers. That is, electron density profiles of these bilayers indicate that the observed break in the pressure–spacing relation occurs at a bilayer separation where extended head groups from apposing bilayers come into steric hindrance. The pressure–spacing data are used to separate steric pressure from the repulsive hydration pressure, as well as to quantitate the range and magnitude of the steric interaction. An appreciable fraction of the measured steric energy can be ascribed to a decrease in configurational entropy due to restricted head-group motion as adjacent bilayers come together.

The close approach of surfaces separated by solvent is opposed by several types of repulsive pressures, including electrostatic, hydration, and steric pressures. The first two of these have been studied extensively. Electrostatic interactions between charged surfaces can be explained in terms of classical double-layer theory (Verwey & Overbeek, 1948; Israelachvili & Adams, 1978). The hydration pressure, P_h, which arises from the work of removal of polarized water molecules from between hydrophilic surfaces, has been shown empirically to

† This research was supported by a grant from the National Institutes of Health (GM-27278).

‡ Department of Anatomy.

§ Departments of Anesthesiology and Physiology.

0006-2960/87/0426-7325$01.50/0

decay exponentially with increasing fluid separation between surfaces, d_f (LeNeveu et al., 1976, 1977; Parsegian et al., 1979; Rau et al., 1984; McIntosh & Simon, 1986a). Considerably less experimental data are available concerning steric interactions, even though steric repulsion plays an important role in such diverse phenomena as the stability of colloidal dispersions, protein assembly, and cell–cell interactions (Napper, 1977; Bongrand & Bell, 1984). Most direct measurements of steric pressures between surfaces have been performed with polymers of large radii of gyration absorbed to rigid substrates (Cain et al., 1978; Klein, 1980) and thus cannot provide molecular details of the events occurring as the surfaces come into contact. Such molecular information is necessary to understand in quantitative detail the interactions between surfaces such as lipid bilayers or biological membranes. For these systems, the experimental task is to separate the contributions of steric pressure, P_s, from those of the hydration pressure, P_h (Marra & Israelachvili, 1985).

In this paper, X-ray diffraction structural analysis is applied to egg phosphatidylcholine (EPC)[1] multilayers compressed by vapor pressures, P, up to 2×10^9 dyn/cm^2 (about 2000 atmospheres). By comparing plots of ln P versus both separation between bilayers and water content, we are able to separate the total pressure, P, into its major components. This provides estimates for both the range and magnitude of steric interactions between EPC bilayers. It is found that, whereas the hydration pressure, as modified by thermal–mechanical fluctuations (Harbich & Helfrich, 1984; Schneider et al., 1984; Evans & Parsegian, 1986), is the dominant repulsive interaction for water contents in the range of 23–10 water molecules per lipid molecule, P_s becomes the largest pressure at lower water contents. Both the hydration and steric barriers may be important factors in hindering the fusion of vesicles containing phosphatidylcholine (PC).

Materials and Methods

Egg phosphatidylcholine in chloroform solution (20 mg/mL) was obtained from Avanti Polar Lipids, Inc., gave a single spot by thin-layer chromatography (TLC), and was used without further purification. TLC was performed on silica G plates using 100-μg loads (first dimension, chloroform:methanol:water, 20:20:1 v/v/v; second dimension, chloroform:methanol:ammonium hydroxide, 65:25:5). Oriented lipid multilayers were prepared by placing a small (about 20 μL) drop of the EPC/chloroform solution on a flat piece of aluminum foil and evaporating the chloroform under a stream of nitrogen. The aluminum foil substrate was given a convex curvature by bending it around a Pasteur pipet. The specimen was then mounted in a controlled humidity chamber on a single-mirror (line-focused) X-ray camera, such that the X-ray beam was oriented at a grazing angle relative to the multilayers on the convex surface of the foil. The specimen curvature and camera geometry ensure that lamellar diffraction to an equivalent Bragg spacing of about 5 Å can be detected (Herbette et al., 1977). The humidity chamber consisted of a copper canister with two Mylar windows for passage of the X-ray beam. Relative humidity was controlled in the chamber by means of a cup of either a saturated salt or a glycerol/water solution at the base of the canister. To speed equilibration, a very gentle stream of nitrogen gas was passed through a flask of the saturated salt or glycerol solution and then through the chamber. After each X-ray exposure, the cup in the canister was checked to ensure that the salt solution was still saturated (crystals of salt present) or that the glycerol solution was at its initial concentration. Glycerol concentrations were checked by refractive index measurements on an Abbé refractometer. The inside of the humidity chamber, as well as the external flask, was kept at 20 ± 1 °C for all experiments.

X-ray diffraction patterns were recorded on a stack of four sheets of Kodak DEF X-ray film in a flat plat film cassette. X-rays were obtained from a Jarrell-Ash Microfocus X-ray generator, and exposure times were on the order of 4–8 h. Specimen-to-film distance was determined to be 10.5 ± 0.1 cm by the use of lead stearate as a calibration standard. X-ray films were processed by standard methods, and a densitometer trace through the center of each reflection was obtained with a Joyce-Loebl Model MKIIIC microdensitometer. After background subtraction, integrated intensities, $I(h)$, were obtained for each order h by measuring the area under the peak. Each intensity $I(h)$ was multiplied by h (the Lorentz correction factor) due to the cylindrical curvature of the multilayers (Blaurack & Worthington, 1966; Herbette et al., 1977; McIntosh, 1978). For these line-focused patterns there was no detectable arcing of the reflections, which were of uniform height. Therefore, no other correction factor was applied and the structure amplitude of order h was set equal to $[hI(h)]^{1/2}$. The validity of this correction factor was demonstrated by the fact that the structure amplitudes for the high humidities (98% and 93% relative humidity) fell on the same continuous transform as obtained for unoriented dispersions of EPC at equivalent applied osmotic pressures (Figure 1; McIntosh & Simon, 1986a). Moreover, the electron density profiles for these humidities are very similar to those of unoriented bilayers subjected to equivalent osmotic pressures (see Figure 3). Electron density profiles were calculated by

$$\rho(x) = \frac{1}{d}\sum \exp(i\phi(h))[hI(h)]^{1/2} \cos \frac{2\pi h x}{d} \qquad (1)$$

where d is the lamellar repeat period and $\phi(h)$ is the phase angle, either 0 or π, for each order h. For these experiments, the phase angles determined by Torbet and Wilkins (1976) were used. Each unit cell contains one bilayer plus the fluid space between adjacent bilayers. That is, $d = d_b + d_f$, where d_b is the bilayer width and d_f is the width of the fluid space.

The ratio of the vapor pressure (p) of various saturated salt or glycerol solutions to the vapor pressure of pure water, p_0, has been previously determined (Grover & Nicol, 1940; O'Brien, 1948; Weast, 1984). The following saturated salt and glycerol solutions were used to obtain the indicated relative vapor pressures (p/p_0): $CuSO_4$ (0.98), Na_2SO_4 (0.93), KCl (0.87), NH_4Cl (0.80), $NaNO_3$ (0.66), $Na_2Cr_2O_7 \cdot 2H_2O$ (0.52), $CaCl_2$ (0.32), $KC_2H_3O_2$ (0.20), LiCl (0.15), 20% glycerol (0.94), 60% glycerol (0.74), and 90% glycerol (0.22). The pressure, P, applied to the EPC specimens is related to μ_w, the chemical potential difference between the interlamellar water and the bulk water phase, by $P = -\mu_w/V_w$, where V_w is the partial molar volume of water (Parsegian et al., 1979). The applied pressure is given by

$$P = -(RT/V_w) \ln (p/p_0) \qquad (2)$$

where R is the molar gas constant and T is temperature. In the data presented in this paper, v_w was set equal to its value in bulk solution, 18 cm^3/mol (Le Neveu et al., 1977; Parsegian et al., 1979). The increase in free energy necessary to change the volume of interlamellar water by an amount ΔV_w is given by $-P\Delta V_w$. As described by Parsegian et al. (1979), this free energy can be parceled into the work of bilayer deformation and the work to decrease the fluid separation between bilayers.

[1] Abbreviations: EPC, egg phosphatidylcholine; PC, phosphatidylcholine.

In particular, the work to bring bilayers together by an incremental amount Δd_f is equal to $-PA(\Delta d_f)/2$, where A is the area per lipid molecule.

The number of water molecules per lipid as a function of P was calculated by a method similar to that described by LeNeveu et al. (1977). EPC, obtained in lyophilized form from Avanti, was placed in a polypropylene container whose weight had previously been measured. Since EPC is hygroscopic, the lipid and open container were dried under vacuum overnight over phosphorus pentoxide. The vacuum chamber was purged with dry nitrogen and the container quickly closed and reweighed, thus providing the dry weight of the lipid. A given amount of water was added and the lipid/water weight measured. After incubation for 24 h, the lipid/water suspensions were sealed in quartz capillary tubes and X-ray diffraction patterns recorded. The lamellar repeat period was then compared to our previously obtained data of ln P as a function of repeat period (McIntosh & Simon, 1986a; and also see Figure 1) to give ln P as a function of water content. It should be noted that this method is not applicable for $P \geq 6 \times 10^7$ dyn/cm^2, where d is nearly invariant with pressure (Figure 1). However, for these high pressures water adsorption isotherms have been obtained for EPC by Jendrasiak and Hasty (1974), Elworthy (1961), and Lundberg (1974). These three adsorption isotherms are in general agreement, and we have chosen to use the data of Jendrasiak and Hasty (1974) since their method of specimen preparation was most similar to ours.

Results

For relative humidities in the range of 22–98% each X-ray diffraction pattern of EPC consisted of a broad wide-angle reflection centered at about 4.5 Å and a series of low-angle reflections, which indexed as orders of a single lamellar repeat period. For this range of relative humidities the lamellar repeat periods were between 49 and 53 Å. These patterns are characteristic of multilayers of liquid-crystalline bilayers (Tardieu et al., 1973). At 20% and 15% relative humidities, additional sharp reflections were observed which indexed as orders of a lamellar repeat of about 57 Å. The reflections of this 57-Å repeat were quite weak at 20% relative humidity, but much stronger at 15% relative humidity. In addition, for both of these two lower humidities, sharp wide-angle reflections were observed at 4.2 Å. This indicates that at 20% and 15% relative humidities a gel phase is observed in addition to the liquid-crystalline phase. Phase diagrams show that EPC is found in the gel phase at very low water contents (Reiss-Husson, 1967; Small, 1986). Thus, 20% and 15% relative humidities correspond to water contents at the boundary between the gel and liquid-crystalline regions of the phase diagram. On the basis of the relative magnitude of the recorded intensities, it appears that the liquid-crystalline phase is the predominant phase present at 20% relative humidity, whereas the gel phase is the predominant phase present at 15% relative humidity. In this paper we consider only the liquid-crystalline phase.

Figure 1 shows the natural logarithm of applied pressure (ln P) plotted against the repeat period (d) for EPC bilayers. Data are included from three laboratories, including our own (Parsegian et al., 1979; Torbet & Wilkins, 1976; McIntosh & Simon, 1986a). This plot is linear from $d \cong 61$ Å to $d \cong 51$ Å, with sharp breaks at both ends of the curve. The linear region of the curve has been equated to the repulsive "hydration" pressure, P_h, caused by the work of removal of water from between the bilayer surfaces (LeNeveu et al., 1977; Parsegian et al., 1979; Marra & Israelachvili, 1985; McIntosh & Simon, 1986a), although a recent theoretical analysis indicates that thermal–mechanical fluctuations may contribute an "undulation" or "fluctuation" pressure, P_f (Evans & Parsegian, 1986). In this region of the curve, bilayer thickness (d_b) remains approximately constant (McIntosh & Simon, 1986a), so that the reduction in d with increasing pressure is due to a reduction in fluid thickness (d_f). The break at the low-pressure end of the curve is due to the fact that, near the equilibrium separation in excess water ($d \cong 63$ Å), the van der Waals attractive pressure becomes comparable in magnitude to the hydration pressure, resulting in a downward deflection in the pressure versus spacing curve (LeNeveu et al., 1977). The sharp upward break in the plot (Figure 1), which begins at ln $P \cong 18$ and $d \cong 51$ Å, was first noted by White and King (1985) and is the primary focus of the experiments in Figures 2–4.

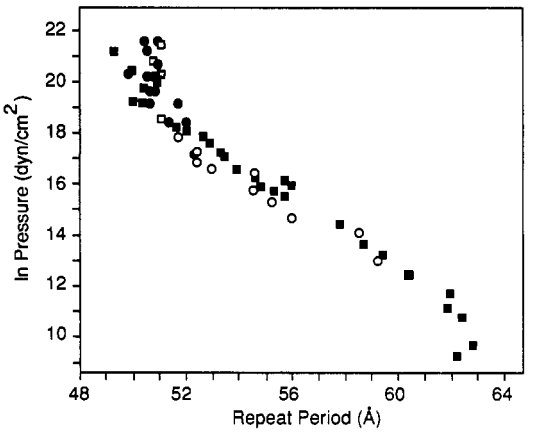

FIGURE 1: Natural logarithm of applied osmotic and vapor pressures, ln P, plotted versus the lamellar repeat period, d. This figure shows the data of Parsegian et al. (1979) (solid squares) and Torbet and Wilkins (1976) (open squares), as well as our osmotic (McIntosh & Simon, 1986a) (open circles) and vapor pressure data (solid circles).

Three causes could be postulated for this observed upward break at $d \cong 51$ Å in Figure 1: (1) a discontinuity in P_h, that is, an abrupt increase in the energy required to remove water from between bilayers at low water content, (2) a 5–6-Å increase in bilayer thickness occurring for $d \leq 51$ Å (so that the increase in d_b would compensate for the decrease in d_f), and (3) the onset of steric repulsion between lipid head groups from opposing bilayers. The data presented in Figures 2–4 provide evidence that the first two possibilities cannot fully explain the data and show that this break occurs at a bilayer separation where the onset of steric hindrance would be expected. Possibility 1 can be excluded since the pressure required to remove water is an exponential function of water content and has no apparent discontinuities from 23 to 2 waters per lipid molecule (Figure 2). Possibility 2 cannot account, by itself, for the observed break since electron density profiles (Figure 3) show that there is only about a 2-Å increase in bilayer thickness for the entire range d = 50–59 Å. In the electron density profiles in Figure 3 the low-density trough at 0 Å corresponds to the terminal methyl groups in the geometric center of the bilayer, the highest density peaks located at about ±20 Å correspond to the lipid head groups, the medium-density regions between the terminal methyl trough and the head-group peaks correspond to the methylene chains, and the medium-density regions at the outer edges of each profile correspond to half of the fluid space between adjacent bilayers. The fluid space is widest at the lowest applied pressure and decreases as the applied pressure increases. The distance between the high density head group peaks across the bilayer remains constant (to within ±1 Å) for the repeat-period range d = 59 Å (ln P = 12.9) to d

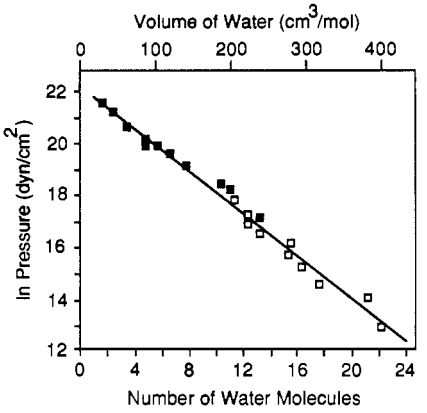

FIGURE 2: Natural logarithm of applied pressure plotted versus the number of water molecules per lipid molecule. The solid squares are taken from the adsorption isotherms of Jendrasiak and Hasty (1974), and the open squares are taken from our X-ray phase diagram of EPC in water by the method of LeNeveu et al. (1977). The top scale indicates the volume of water per mole of lipid, assuming that the molar volume of a water molecule is 18 cm^3/mol.

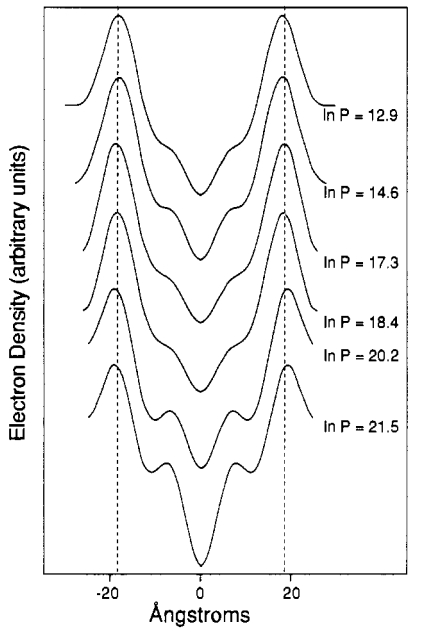

FIGURE 3: Electron density profiles for EPC bilayers for the range of applied pressures of 4×10^5 dyn/cm^2 (ln P = 12.97) to 2.3×10^9 dyn/cm^2 (ln P = 21.5). The top three profiles are from unoriented liposomes in PVP solutions (McIntosh & Simon, 1986a), and the botton three profiles are from oriented multilayers in controlled relative humidity atmospheres. The pair of dotted lines denote the average head group peak separation for profiles for ln P <18 (McIntosh & Simon, 1986a).

= 52 Å (ln P = 17.3) as previously reported (McIntosh & Simon, 1986a). For d less than 52 Å, detectable structural changes occur in the bilayer as further water is removed. That is, the bilayers shown in Figure 3 for ln $P \cong$ 21.5 and 20.3 are about 2 Å wider than the bilayers at the lower applied pressures. Moreover, the terminal methyl trough becomes progressively sharper and deeper at these higher pressures. This is due to a higher degree of localization of the terminal methyl groups in the bilayer center as the area per molecule (A) decreases.

The profiles shown in Figure 3 and profiles obtained at the other applied pressures shown in Figure 1 can be used to estimate the width of the fluid space between adjacent bilayers (McIntosh & Simon, 1986a). As noted by Marra and Israelachvili (1985), the definition of fluid thickness is somewhat arbitrary, since (1) the bilayer surface is not molecularly

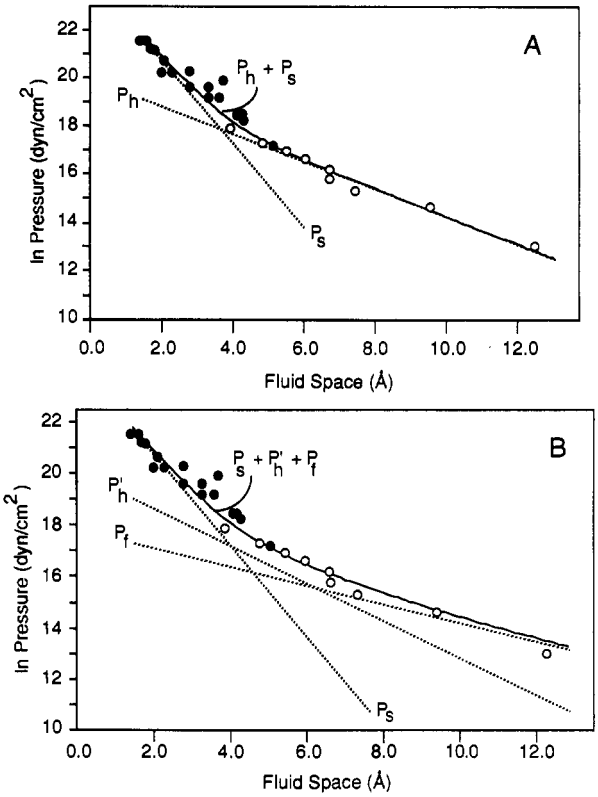

FIGURE 4: Natural logarithm of applied pressure (ln P) in dynes per square centimeter plotted versus the fluid space d_f between adjacent bilayers obtained from electron density profiles. The open circles represent data from osmotic pressure experiments (McIntosh & Simon, 1986a), and the closed circles represent data from vapor pressure experiments. In (A) the dotted lines are the hydration pressure $P_h = 4.7 \times 10^8 \exp(-d_f/1.7)$ and the steric pressure $P_s = 3.6 \times 10^{10} \exp(-d_f/0.6)$, and the solid line is $P_s + P_h$. In (B) the hydration pressure was recalculated to take into account the fluctuation pressure, P_f. The dotted lines show $P_h' = 5.1 \times 10^8 \exp(-d_f/1.4)$, $P_s = 3.6 \times 10^{10} \exp(-d_f/0.6)$, and $P_f = 5.4 \times 10^7 \exp(-d_f/2.8)$, and the solid line is the sum $P_h' + P_s + P_f$.

smooth, (2) the polar head groups are mobile (Hauser, 1981), (3) the entire bilayer undergoes thermal undulations (Harbich & Helfrich, 1984), and (4) water penetrates into the lipid head group region (Worcester & Franks, 1976; Büldt et al., 1979; Simon et al., 1982). As we have done previously (McIntosh & Simon, 1986a), we operationally define the bilayer width as the total thickness of the bilayer assuming that the headgroup conformation is the same in EPC as it is in single crystals of dimyristoylphosphatidylcholine (Pearson & Pascher, 1979). That is, in this definition it is assumed that the phosphocholine group is oriented approximately parallel to the bilayer plane. The electron density peaks in the profiles in Figure 3 are located near the center of the head group, that is, between the phosphate moiety and the glycerol backbone (Lesslauer et al., 1972; Hitchcock et al., 1974). From space-filling models, this places these electron density peaks about 5 Å inward from the edge of the bilayer when the head group is oriented parallel to the bilayer plane. Therefore, the bilayer thickness, d_b, is set equal to the distance between electron density peaks in the profiles (Figure 3) plus 10 Å (McIntosh & Simon, 1986a). The fluid thickness, d_f, is then calculated from $d_f = d - d_b$.

Figure 4A shows ln P plotted versus d_f. For d_f = 5–12 Å the plot is linear and has been equated to the hydration pressure, P_h (McIntosh & Simon, 1986a). The dotted line in Figure 4A labeled P_h is a least-squares fit to the data for 5 Å $< d_f <$ 12 Å and is $P_h = P_{h_0} \exp(-d_f/\lambda)$, where $P_{h_0} = 4.7 \times 10^8$ dyn/cm^2 and λ = 1.7 Å. For d_f <5 Å, the data points lie significantly above this line. That is, even after the changes

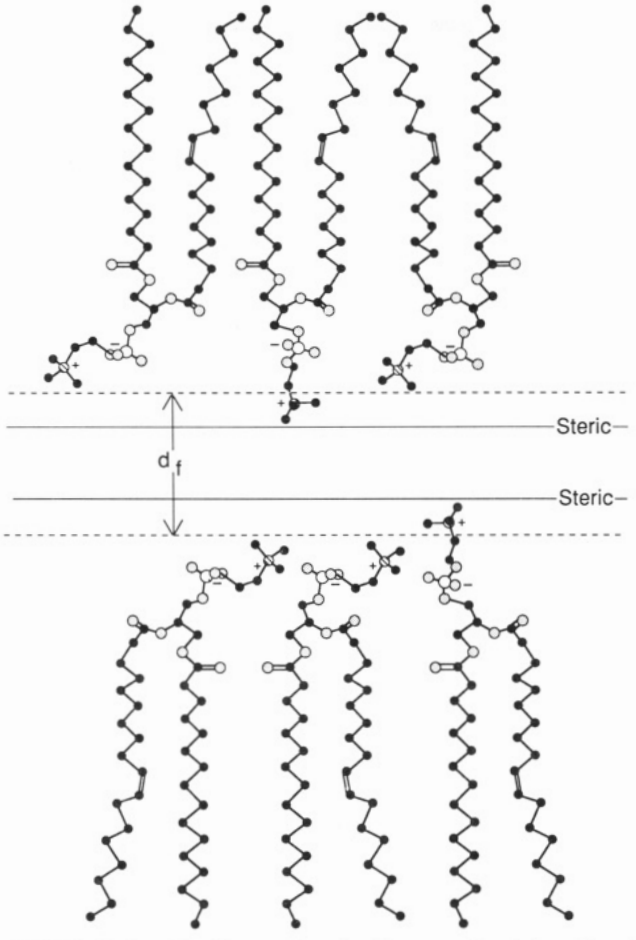

FIGURE 5: Schematic diagram showing the approximate location of the plane where steric interactions are first observed for EPC (solid line). The dotted lines delimit the fluid space, d_f, as determined by electron density profiles, assuming the parallel orientation of the lipid head groups. The head groups rotate so that trimethylammonium moieties extend 2–3 Å into the fluid space. Depicted are the two extremes of head-group orientation, with the phosphocholine moiety parallel and perpendicular to the plane of the bilayer (Hauser, 1981).

in bilayer thickness are accounted for by the procedure described above, a break in ln P versus d_f still remains.

The position of the observed break in Figure 4A can be explained in terms of steric interactions. That is, the value of $d_f = 5$ Å for the onset of steric repulsion is consistent with the NMR data of Hauser (1981) which indicate that the phosphocholine group rotates from its preferred position, approximately parallel to the bilayer, to a position where it extends 2–3 Å farther into the fluid space (see Figure 5). Thus, on the basis of Hauser's model for head-group motion, trimethylammonium group from apposing bilayers would be expected to come into steric hindrance at $d_f \simeq 4$–6 Å. Local variations in bilayer thickness, or "breathing" modes, would tend to "soften" the edge of the steric barrier and could extend the range of steric interactions.

By analytical continuation, P_h can be extended from $d_f = 5$ Å to $d_f = 1.5$ Å (dotted line labeled P_h in Figure 4A). The total pressure (P) can then be separated into two major components, P_h and steric pressure, P_s. That is, in Figure 4A the two dotted lines correspond to P_h and P_s and the solid line corresponds to the sum of $P_h + P_s$. A least-squares fit to the data points is found with $P_s = P_{s_0} \exp(-d_f/\alpha)$, where $P_{s_0} = 3.6 \times 10^{10}$ dyn/cm^2 and $\alpha = 0.6$ Å. A single exponential function is used for P_h in the range $d_f \simeq 1.5$–13 Å. Alternatively, P_h could be set equal to $(P_{h_0}/4)\ \mathrm{sech}^2\ (d_f/2\lambda)$ for $d_f \leq \lambda$ (Cevc and Marsh, 1985). However, since $P_s \gg P_h$ for $d_f \leq \lambda$, this refinement would make little difference in calculations of P_s. For P_s, an exponential function provides a good fit for the data in the range of $d = 1.5$–5 Å. However, since this range of separations is small, other functional forms, such as power laws or polynomials, could also be used.

In Figure 4B a similar procedure is followed, except that the effects of thermal–mechanical fluctuations, or thermally induced bending of the bilayer sheets, are included, following the formalism of Evans and Parsegian (1986). These fluctuations are theoretically predicted by Evans and Parsegian (1986) to give rise to a pressure of the form

$$P_f = (\pi KT/32\lambda')(P_{h_0}'/B\lambda')^{1/2} \exp(-d_f/2\lambda') \qquad (3)$$

where B is the bilayer bending modulus, which is about 10^{12} erg (Servuss et al., 1978; Lorenzen et al., 1986) and P_{h_0}' and λ' are the parameters in the hydration pressure modified to take into account the thermal undulations. One effect of including thermal fluctuations in the analysis is that it decreases the value of λ in P_h (Evans & Parsegian, 1986). Our procedure was to set λ' equal to 1.4 Å, the value for gel-state phosphatidylcholine bilayers (McIntosh & Simon, 1986a) where thermal fluctuations are negligible. Thus, when fluctuations are included, $P_h' = Ph_{h_0}' \exp(-d_f/1.4)$ and $P_f = (\pi KT/32\lambda')(P_{h_0}'/\lambda' B)^{1/2} \exp(-d_f/2.8)$, where the only unknown parameter is P_{h_0}'. A value of $P_{h_0}' = 5.1 \times 10^8$ dyn/cm^2 is obtained from a least-squares fit to the experimental data points for $d_f > 5$ Å. The calculated pressures P_f and P_h', along with P_s as given above, are shown as dotted lines in Figure 4B. The solid line corresponds to the sum $P_s + P_h' + P_f$. It can be seen that, with the same value for P_s, the data points can be fit either with (Figure 4B) or without (Figure 4A) a term due to thermal fluctuations.

The work of removing water from EPC bilayers has several components. The energy contributions of the steric (E_s), hydration (E_h), and fluctuation (E_f) interactions can be obtained by integrating P_s, P_h, and P_f from $d_f = 12.4$ Å (ln P = 12.9) to $d_f = 1.4$ Å (ln P = 21.5). These calculations give $E_s \cong 19.3$ erg/cm^2 and $E_h \cong 3.6$ erg/cm^2 when undulations are not included (Figure 4A) and $E_s \cong 19.3$ erg/cm^2, $E_f \cong 0.9$ erg/cm^2, and $E_h' \cong 2.5$ erg/cm^2 when undulations are included (Figure 3B). The energy due to lateral deformation of the bilayer is given by $E_d = 1/2\ K\ (\Delta A/A)^2$, where K is the elastic area compressibility modulus and $\Delta A/A$ is the relative change in area per molecule. The compressibility modulus has been measured to be 140 dyn/cm for fully hydrated EPC bilayers (Kwok & Evans, 1981). If it is assumed that the volume of the bilayer remains constant (LeNeveu et al., 1977; Parsegian et al., 1979), then $\Delta A/A = -\Delta H/H$, where H is the width of the bilayer hydrocarbon region. Following the method of McIntosh and Simon (1986b), we use the electron density profiles of Figure 3 to estimate $-\Delta H/H \simeq 0.1$. This gives $E_d \cong 0.8$ erg/cm^2. This value for the energy of bilayer deformation should be considered a lower bound, since the compressibility modulus could be somewhat higher for partially hydrated bilayers as compared to fully hydrated bilayers and since there might be small bilayer volume changes at low hydration.

For this same pressure range, the total energy (E_t) of removing water from these multilayers can be calculated, independent of any model, from the data presented in Figure 2. Integration of the line in Figure 2 from 23 water molecules per lipid (ln P = 12.9) to 2 water molecules per lipid (ln P = 21.5) gives $E_t \simeq 9.8 \times 10^{10}$ erg/mol $\simeq 51.1$ erg/cm^2, or about 4 times the thermal energy, RT. The conversion from energy per mole to energy density was made by setting $A = 67$ Å^2 for ln $P = 12.9$–18.0 (McIntosh & Simon, 1986a) and

$A = 62$ Å^2 for ln P = 18.0–21.5, as calculated from $\Delta A/A = \Delta H/H \cong 0.1$ (see above).

Discussion

In excess water, the equilibrium separation between neutral membranes, such as EPC bilayers, is determined by a balance between the van der Waals attraction and the repulsive hydration and fluctuation pressures (LeNeveu et al., 1977; Parsegian et al., 1979; Evans & Parsegian, 1986). When EPC bilayers are squeezed together by applied pressures, water is removed from between adjacent bilayers. For applied pressures in the range of 2×10^5 to 6×10^7 dyn/cm^2 ($12 \leq \ln P \leq 17$) plots of ln P versus (1) X-ray repeat period, (2) number of water molecules per lipid, and (3) fluid space between adjacent bilayers are all approximately linear (Figures 1, 2, and 4). In addition, over this pressure range the width of the bilayer and therefore the area per lipid molecule are nearly constant (McIntosh & Simon, 1986a; Figure 3). This indicates that as water is removed from between adjacent bilayers the bilayer surfaces come together by a distance proportional to the volume of water removed (i.e., $\Delta d_f = \Delta V_w/A$, where ΔV_w is the volume of water removed).

However, for applied pressures larger than 3×10^7, dyn/cm^2, a sharp break is present in a plot of ln P versus d (Figure 1) without a corresponding break in ln P versus number of water molecules (Figure 2). The analysis presented under Results indicates that there are two primary causes for this deviation: (1) steric hindrance between the mobile lipid head groups which extend into the fluid space and (2) a relatively small increase (about 2 Å) in bilayer thickness. This estimate for the increase in bilayer thickness is subject to experimental uncertainty due to the limited resolution of the electron density profiles in Figure 3 ($d/2h_{max} \simeq 5.5$ Å). However, since we are measuring changes in the position of two widely spaced and well-defined peaks, namely, the electron-dense head-group peaks, this resolution is sufficient so that changes in bilayer thickness greater than about 1 Å can be detected (McIntosh & Simon, 1986a). The measurements are quite reproducible, with standard deviations in d_f of less than 1 Å [see Figure 4 and McIntosh and Simon (1986a)]. Moreover, our measured changes in bilayer thickness are very similar to those observed in higher resolution electron density profiles by Torbet and Wilkins (1976) and analyzed in detail by White and King (1985). Another potential source of error in our approach is the effect of head-group conformation on the location of the electron density peaks in the profiles. These peaks are due primarily to the electron-dense phosphate moiety and glycerol backbone (Lesslauer et al., 1972). From the analysis of head-group motion by Hauser (1981), it can be seen that the distances from the center of the bilayer for both the phosphate moiety and the glycerol backbone are essentially unchanged for the extremes of head-group positions (Figure 5). Thus, relative to the bilayer center, the position of the high-density peaks in the electron density profiles will be very nearly the same for the range of head-group conformations depicted in Figure 5, and any change in peak-to-peak separation in these profiles (Figure 3) must be primarily attributable to changes in hydrocarbon thickness (McIntosh & Simon, 1986b). We conclude that the abrupt change in slope observed in Figure 4A is real, as it is too large to arise from the sources of uncertainty described above. However, since the pressures P_s, P_h, and P_f are all exponential functions, the calculations of E_s, E_h, and E_f are extremely sensitive to the value of the lower integration limit of d_f. For example, an 0.5-Å difference in the lower values of d_f can cause about a 25% difference in the calculated values of E_s and E_h.

The calculations presented under Results indicate that a relatively small amount of work goes into deforming the bilayer as compared to the work necessary to overcome steric repulsion. In terms of water molecules removed, this analysis indicates that from about 23 to 10 water molecules per lipid molecule the major energy contribution comes from the hydration pressure, perhaps as modified by thermal–mechanical fluctuations, whereas from about 10 to 2 water molecules per lipid much of the work goes to overcome steric repulsion. That is, since water is intercalated between lipid head groups in each monolayer (Worcester & Franks, 1976; Büldt et al., 1979; Simon et al., 1982), apposing bilayers come into steric hindrance before complete dehydration is reached.

There are several mechanisms that might contribute to the steric pressure, P_s. One is the loss of possible head-group conformations due to the close approach of apposing bilayers. For PC micelles, there is nearly free rotation of the head group around the C2–C3 glycerol bond (Hauser, 1981). This same head-group motion likely occurs in fully hydrated bilayers (Hauser, 1981), and so the phosphocholine group is approximately perpendicular to the bilayer plane about one-third of the time and parallel to this plane about two-thirds of the time (Figure 5). However, when apposing bilayers come into contact, the probability of the head group being in the perpendicular conformation decreases. The energy change for total loss of the perpendicular head-group conformation is $E \cong RT \ln (2/3) \cong 0.24$ kcal/mol or about 5.6 erg/cm^2. Thus, conformational entropy can account for most of E_s until very small separations are reached ($d_f \lesssim 2$ Å), whereupon other processes, such as elastic compression (Napper, 1977), may become significant. Another possible contributing factor is surface density variations, which give rise to local changes in bilayer thickness, that is, breathing modes.

For the relative humidity experiments the applied pressure is inversely proportional to the partial molar volume of water, V_w (see Materials and Methods). It is common practice to set V_w equal to 18 cm^3/mol, the molar volume of bulk water (LeNeveu et al., 1977; Parsegian et al., 1979), as we have done in our calculations. However, White and King (1985) have analyzed the data of Torbet and Wilkins (1976) and concluded that V_w becomes significantly less than 18 cm^3/mol for bilayers at low water contents. It should be noted that, in our experiments and in those of LeNeveu et al. (1977) and Parsegian et al. (1979), pressure has been applied to the multilayers by two independent methods—through the vapor phase and by equilibration in a polymer solution. The osmotic pressures of the polymer solutions, which do not depend on V_w, have been directly measured (Vink, 1971; LeNeveu et al., 1977; Parsegian et al., 1986). Fortunately, for the purpose of comparison, there is a range of pressures where the two techniques overlap. That is, 60% poly(vinylpyrrolidone) produces a larger pressure (ln P = 17.9) than does a 98% relative humidity atmosphere (ln P = 17.2, calculated with V_w = 18 cm^3/mol). The measured quantities d (Figure 1), number of water molecules (Figure 2), and fluid thickness (Figure 4A) all fall on continuous lines in this overlap range when V_w is set equal to 18 cm^3/mol. Thus, at least for the highest relative humidities, there is good evidence that $V_w \cong 18$cm^3/mol and that oriented and unoriented bilayers behave similarly. For oriented EPC bilayers at low relative humidities the precise value of V_w is still an open question as it has not been directly measured. However, even if V_w were significantly smaller than 18 cm^3/mol at low relative humidities, the effect would be to increase ln P by the same amount in Figures 1, 2, and 4 in the high-pressure range. Thus, none of the basic arguments

concerning steric interaction would change, although the magnitudes of P_s and E_s would be increased by an amount proportional to the relative decrease in V_w. Note, however, that the value of E_t calculated from the vapor pressure data in Figure 2 is independent of the value of V_w.

An interesting aspect of these energy calculations is that the sum of $E_s + E_h + E_f + E_d$ does not add up to the total energy (E_t) of removing water as calculated from the data in Figure 2. There are several factors that might contribute to this difference. First, as discussed above, is the possibility that V_w might be less than 18 cm^3/mol at low water contents, where the water is strongly attracted to the polar lipid head group (White & King, 1985). Second, is the effect of defects, such as screw dislocations, which are common in these types of lipid multilayers (Kleman et al., 1977). The energy to form an individual screw dislocation can be appreciable and is inversely proportional to the square of the dislocation radius (Zasadzinski, 1986), which is a function of water content. Unfortunately, the density of dislocations at low water contents is difficult to quantitate and so is their energy contribution. Another, and perhaps more important, factor concerning defects is that since they are regions of high energy they can act as collection points for water at low relative humidities. That is, when adjacent bilayers come into steric contact, water molecules will interact to minimize the free energy of the defects. Such water, localized in screw dislocations or other defects, will not be detected in the X-ray experiments. Thus, the energy to remove the water from defects will contribute to E_t as calculated from the data in Figure 2 but is not included in E_s, E_f, E_h, or E_d.

The X-ray data indicate that the EPC hydrocarbon chains crystallize at about 20% relative humidity. This phase change may account for the abrupt deflection in the water adsorption isotherm at this humidity (Jendrasiak & Hasty, 1974).

Finally, it has been observed that bilayers containing significant amounts of phosphatidylcholine fuse at a much lower rate than bilayers containing phosphatidylethanolamine (Düzgünes et al., 1981). The trimethylammonium group of the PC head group might lower the probability of bilayer fusion in two ways: first, by causing steric hindrance, as described in this paper, and, second, by preventing the hydrogen bonding that has been proposed to occur between adjacent PE bilayers (McIntosh & Simon, 1986b).

Acknowledgments

We thank Drs. M. J. Costello, V. A. Parsegian, R. P. Rand, and S. H. White for helpful discussions, Dr. H. P. Erickson for useful suggestions on the calculation of configurational entropy, and Dr. S. M. Gruner for the gift of lead stearate and advice on regulating relative humidity.

Registry No. Choline, 62-49-7.

References

Blaurock, A. E., & Worthington, C. R. (1966) *Biophys. J. 9*, 305–312.

Bongrand, P., & Bell, G. I. (1984) in *Cell Surface Dynamics: Concepts and Models* (Perelson, A. S., Delisi, C., & Wiegel, F. W., Eds.) pp 459–493, Marcel Dekker, New York.

Büldt, G., Gally, H. U., Seelig, J., & Zaccai, G. (1979) *J. Mol. Biol. 134*, 673–691.

Cain, F. W., Ottewill, R. H., & Smitham, J. B. (1978) *Faraday Discuss. Chem. Soc. 65*, 33–42.

Cevc, G., & Marsh, D. (1985) *Biophys. J. 47*, 21–31.

Cowley, A. C., Fuller, N. L., Rand, R. P., & Parsegian, V. A. (1978) *Biochemistry 17*, 3163–3168.

Düzgünes, N., Wilshut, T., Fraley, R., & Papahadjopoulos, D. (1981) *Biochim. Biophys. Acta 642*, 182–195.

Elworthy, P. H. (1961) *J. Chem. Soc.*, 5385–5389.

Evans, E. A., & Parsegian, V. A. (1986) *Proc. Natl. Acad. Sci. U.S.A. 83*, 7132–7136.

Grover, D. W., & Nicol, J. M. (1940) *J. Soc. Chem. Ind., London 59*, 175–177.

Harbich, W., & Helfrich, W. (1984) *Chem. Phys. Lipids 36*, 39–63.

Hauser, H. (1981) *Biochim. Biophys. Acta 646*, 203–210.

Herbette, L., Marquardt, J., Scarpa, A., & Blasie, J. K. (1977) *Biophys. J. 20*, 245–272.

Hitchcock, P. B., Mason, R., Thomas, K. M., & Shipley, G. G. (1974) *Proc. Natl. Acad. Sci. U.S.A. 71*, 3036–3040.

Israelachvili, J. N., & Adams, G. E. (1978) *J. Chem. Soc., Faraday Trans, 1 74*, 975–1001.

Janiak, M. J., Small, D. M., & Shipley, G. G. (1979) *J. Biol. Chem. 254*, 6068–6078.

Jendrasiak, G. L., & Hasty, J. H. (1974) *Biochim. Biophys. Acta 337*, 79–91.

Klein, J. (1980) *Nature (London) 288*, 248–251.

Kleman, M., Williams, C., Costello, M. J., & Gulik-Kryzwicki, T. (1977) *Philos. Mag. 35*, 33–46.

Kwok, R., & Evans, E. (1981) *Biophys. J. 35*, 637–652.

LeNeveu, D. M., Rand, R. P., & Parsegian, V. A. (1976) *Nature (London) 259*, 601–603.

LeNeveu, D. M., Rand, R. P., Parsegian, V. A., & Gingell, D. (1977) *Biophys. J. 18*, 209–230.

Lesslauer, W., Cain, J. E., & Blasie, J. K. (1972) *Proc. Natl. Acad. Sci. U.S.A. 69*, 1499–1503.

Lorenzen, S., Servuss, R.-M., & Helfrich, W. (1986) *Biophys. J. 50*, 565–572.

Lundberg, B. (1974) *Acta Chem. Scand., Ser. B B28*, 673–676.

Luzzati, V. (1968) in *Biological Membranes* (Chapman, D., Ed.) pp 71–123, Academic, New York.

Marcelja, S., & Radic, N. (1976) *Chem. Phys. Lett. 42*, 129–130.

Marra, J., & Israelachvili, J. (1985) *Biochemistry 24*, 4608–4618.

McIntosh, T. J. (1978) *Biochim. Biophys. Acta 513*, 43–58.

McIntosh, T. J., & Simon, S. A. (1986a) *Biochemistry 25*, 4058–4066.

McIntosh, T. J., & Simon, S. A. (1986b) *Biochemistry 25*, 4948–4952.

Napper, P. H. (1977) *J. Colloid Interface Sci. 58*, 390–407.

O'Brien, F. E. M. (1948) *J. Sci. Instrum. 25*, 73–76.

Parsegian, V. A., Fuller, N., & Rand, R. P. (1979) *Proc. Natl. Acad. Sci. U.S.A. 76*, 2750–2754.

Parsegian, V. A., Rand, R. P., Fuller, N. L., & Rao, D. C. (1986) *Methods Enzymol. 127*, 400–416.

Pearson, S. H., & Pascher, I. (1979) *Nature (London) 281*, 499–501.

Rau, D. C., Lee, B. K., Parsegian, V. A. (1984) *Proc. Natl. Acad. Sci. U.S.A. 81*, 2621–2626.

Reiss-Husson, F. (1967) *J. Mol. Biol. 25*, 363–382.

Schneider, M. B., Jenkins, J. T., & Webb, W. W. (1984) *Biophys. J. 45*, 891–900.

Servuss, R. M., Harbich, W., & Helfrich, W. (1978) *Biochem. Biophys. Acta 436*, 900–903.

Simon, S. A., McIntosh, T. J., & Latorre, R. (1982) *Science (Washington, D.C.) 216*, 65–67.

Small, D. M. (1986) *Handb. Lipid Res. 4*, 511.

Tardieu, A., Luzzati, V., & Reman, F. C. (1973) *J. Mol. Biol. 75*, 711–733.

Torbet, J., & Wilkins, M. H. F. (1976) *J. Theor. Biol. 62*, 447–458.
Verwey, E. J. W., & Overbeek, J. Th. G. (1948) *Theory of the Stability of Lyophobic Colloids*, Elsevier, Amsterdam.
Vink, H. (1971) *Eur. Polym. J. 7*, 1411–1419.
Weast, R. C. (1984) *CRC Handbook of Chemistry and Physics, 65th ed.*, p E-42.
White, S. H., & King, G. I. (1985) *Proc. Natl. Acad. Sci. U.S.A. 82*, 6532–6536.
Zasadzinski, J. A. N. (1986) *Biophys. J. 49*, 1119–1130.

Uncoupling of Oxidative Phosphorylation. 1. Protonophoric Effects Account Only Partially for Uncoupling†

Siro Luvisetto, Daniela Pietrobon,*,‡ and Giovanni Felice Azzone
CNR Unit for the Study of the Physiology of Mitochondria and Institute of General Pathology, University of Padova, 35100 Padova, Italy

Received January 21, 1987; Revised Manuscript Received May 8, 1987

ABSTRACT: The mechanism of uncoupling of oxidative phosphorylation by carbonyl cyanide *p*-trifluoromethoxy)phenylhydrazone (FCCP), a typical weak acid protonophore, oleic acid, a fatty acid, and chloroform, a general anesthetic, has been investigated by measuring in mitochondria their effect on (i) the transmembrane proton electrochemical potential gradient ($\Delta\tilde{\mu}_H$) and the rates of electron transfer and adenosine 5′-triphosphate (ATP) hydrolysis in static head, (ii) $\Delta\tilde{\mu}_H$ and the rates of electron transfer and ATP synthesis in state 3, and (iii) the membrane proton conductance. Both FCCP and oleic acid increase the membrane proton conductance, and accordingly, they cause a depression of $\Delta\tilde{\mu}_H$ [generated by either the redox proton pumps or the adenosinetriphosphatase (ATPase) proton pumps]. Although their effects on ATP synthesis/hydrolysis, respiration, and $\Delta\tilde{\mu}_H$ are qualitatively consistent with a pure protonophoric uncoupling mechanism and an additional inhibitory action of oleic acid on both the ATPases and the electron-transfer enzymes, a quantitative comparison between the dissipative proton influx and the rate of either electron transfer or ATP hydrolysis (multiplied by either the H^+/e^- or the H^+/ATP stoichiometry, respectively) at the same $\Delta\tilde{\mu}_H$ shows that the increase in membrane conductance induced by FCCP and oleic acid accounts for the stimulation of the rate of ATP hydrolysis but not for that of the rate of electron transfer. Chloroform (at concentrations that fully inhibit ATP synthesis) only very slightly increases the proton conductance of the mitochondrial membrane and causes only a little depression of $\Delta\tilde{\mu}_H$. The negligible increase in the dissipative proton influx in the presence of chloroform does not account for the stimulation either of the rate of electron transfer or of ATP hydrolysis. The classical "chemiosmotic" explanation of the uncoupling of oxidative phosphorylation does not apply to the uncoupling action of chloroform.

The mechanism by which a number of substances uncouple oxidative phosphorylation, i.e., inhibit ATP[1] synthesis and stimulate resting respiration, has been the subject of intense research. In fact, any hypothesis on the mechanism of free energy coupling (between electron transfer and ATP synthesis) has to provide an explanation for the uncoupling consistent with the known properties of these substances. Thus, the observations that typical lipophilic weak acid uncouplers, such as 2,4-dinitrophenol (DNP) and carbonyl cyanide *p*-(trifluoromethoxy)phenylhydrazone (FCCP), increase the proton conductance of the inner mitochondrial membrane (Mitchell & Moyle, 1967) and of black lipid membranes (Hopfer et al., 1968) have been considered strong evidence in favor of the chemiosmotic hypothesis as formulated by Mitchell (1966).

Much work has been devoted to establishing if the protonophoric action could quantitatively account for the uncoupling of oxidative phosphorylation [for reviews see Hanstein (1976) and McLaughlin and Dilger (1980)]. From these studies it can be generally concluded that certainly there exists a correlation between protonophoric and uncoupling action. However, no clear-cut evidence that the uncoupling is exclusively and quantitatively due to the increase in membrane conductance has ever been reported. In fact, the quantitative comparison between the rate of passive proton influx in the presence of FCCP and the rate of electron transfer multiplied by the H^+/e^- stoichiometry made originally by Mitchell and Moyle (1967) was based on estimated values of $\Delta\tilde{\mu}_H$ and on measured values of H^+/e^- stoichiometries that were much too high for the former and too low for the latter with respect to the actual measurements (Wikstrom & Krab, 1980; Azzone et al., 1984). Instead, preliminary reports from our laboratory

† This work was aided in part by a grant from the Regione Veneto and by a fellowship of ASSNE to S.L.
‡ Present address: Department of Physiology and Biophysics, Harvard Medical School, Boston, MA 02115.

[1] Abbreviations: J_o^{sh}, rate of respiration in static head; J_o^{st3}, rate of respiration in state 3; J_o^{max}, maximal rate of respiration; J_e, rate of electron transfer; J_p, rate of ATP synthesis; J_{ATP}, rate of ATP hydrolysis; J_K^{eff}, rate of K^+ efflux; J_H^l, proton flux through leaks; $\Delta\psi$, transmembrane electrical potential gradient; ΔpH, transmembrane pH gradient; $\Delta\tilde{\mu}_H$, transmembrane proton electrochemical potential gradient (in absolute value); L_H^l, membrane proton-leak conductance; n_e, H^+/e^- stoichiometry; n_p, H^+/ATP stoichiometry; f_e, fraction of active redox pumps; f_p, fraction of active ATPase pumps; P_i, inorganic phosphate; DMO, 5,5-dimethyloxazolidine-2,4-dione; $TPMP^+$, triphenylmethylphosphonium ion; Mops, 3-(*N*-morpholino)propanesulfonic acid; Tris, tris(hydroxymethyl)aminomethane; EDTA, ethylenediaminetetraacetic acid; EGTA, [ethylenebis(oxyethylenenitrilo)]tetraacetic acid; NADH, reduced nicotinamide adenine dinucleotide; NADP, nicotinamide adenine dinucleotide phosphate; FCCP, carbonyl cyanide *p*-(trifluoromethoxy)phenylhydrazone; DCCD, *N*,*N*′-dicyclohexylcarbodiimide; ATP, adenosine 5′-triphosphate; ATPase, adenosinetriphosphatase; ADP, adenosine 5′-diphosphate.

0006-2960/87/0426-7332$01.50/0